J. Biochem. 124, 578-584 (1998)

# Conformational Changes at the Highly Reactive Cystein and Lysine Regions of Skeletal Muscle Myosin Induced by Formation of Transition State Analogues

Shinsaku Maruta,[1] Kazuaki Homma, and Takashi Ohki

*Department of Bioengineering, Faculty of Engineering, Soka University, Hachioji, Tokyo 192-8577*

Received for publication, April 6, 1998

**Myosin forms stable ternary complexes with $Mg^{2+}$-ADP and phosphate analogues of aluminum fluoride ($AlF_4^-$), beryllium fluoride (BeFn), and scandium fluoride (ScFn). These complexes are distinct from each other and may mimic different transient states in the ATPase cycle [Maruta *et al.* (1993) *J. Biol. Chem.* 268, 7093-7100]. Regions of skeletal muscle myosin containing the highly reactive residues Cys 707 (SH1), Cys 697 (SH2), and lysine 83 (RLR) dramatically alter their local conformation when myosin hydrolyzes ATP, and these changes may reflect formation of a series of transient intermediates during ATP hydrolysis. We used the fluorescent probes 4-fluoro-7-sulfamoylbezofurazan, 2-(4′-maleimidylanilino)naphthalene-6-sulfonic acid, and trinitrobenzene-sulfonate, which bind to SH1, SH2, and RLR, respectively, to examine differences in local conformations within myosin·ADP·phosphate analogue (BeFn, $V_i$, $AlF_4^-$, and ScFn) complexes. It was observed that the ternary complexes had SH1 conformations similar to those seen on S-1 in the presence of ATP. In contrast, local conformations in the SH2 and RLR regions of S-1·ADP·BeFn were different from those in corresponding regions of S-1·ADP·$AlF_4^-$ or ScFn. These results suggest that SH1 and SH2 move distinctly during ATP hydrolysis and that the local conformations of the SH2 and RLR regions more sensitively reflect different transient states.**

**Key words: ATP analogues, chemical modification, energy transduction, fluorescent probes, myosin.**

The energy for muscle contraction is generated from the hydrolysis of $Mg^{2+}$-ATP by myosin, a process activated by the binding of actin. During the ATPase cycle, myosin forms a series of transient intermediates including M·ATP, M*·ATP, M**·ADP·$P_i$, and M*·ADP (*1, 2*). Numerous biochemical studies have demonstrated that ATP hydrolysis and formation of the intermediates are accompanied by localized changes in the conformation of the myosin head, *e.g.*, in the regions of Trp 510 (*3-5*), Cys 707-Cys 697 (*6-8*), and Lys 83 (*9-11*). Global changes in the shape of the myosin head during ATP hydrolysis have also been demonstrated using small angle synchrotron X-ray scattering (*12, 13*). Nevertheless, it has proven difficult to study the sequence of conformational changes in myosin because the transient intermediates have only a brief lifetime. Consequently, the precise nature of the conformational changes in the myosin head that are directly related to energy transduction remains unclear.

To study the conformations of the transient intermediates in the ATPase cycle and their roles in energy transduction in detail, stable analogues mimicking the structures of the intermediates would be very useful. Fortunately, in the presence of $Mg^{2+}$-ADP, myosin forms stable ternary complexes with the phosphate analogues beryllium fluoride (BeFn; *14-16*), vanadate ($V_i$; *17*), aluminum fluoride ($AlF_4^-$; *14, 15*), and scandium fluoride (ScFn; *18*), and these complexes appear to mimic transient states of ATP hydrolysis. In addition, we previously demonstrated that the various complexes differ from each other in the way they interact with actin and in their ability to enhance intrinsic tryptophan fluorescence, thus indicating that they do not mimic the same transient state (*14, 19*). Indeed, the conformation of the BeFn complex differs significantly in the region of the C-terminal tail from those of the $AlF_4^-$ and $V_i$ complexes (*21, 22, 23*); their respective structures suggest that the $AlF_4^-$ and $V_i$ complexes may mimic the transition state of M**·ADP·$P_i$, while the BeFn complex mimics the M·ATP state.

At variance with this proposal are small angle X-ray solution scattering studies which indicate that, in either the presence or absence of ATP, all skeletal myosin S-1 complexes have rounded shapes (*12, 13*). But discrepancies with numerous biochemical data, especially with respect to conformational changes at flexible regions of myosin,

[1] To whom correspondence should be addressed. Phone: +81-426-91-9443, Fax: +81-426-91-9312, E-mail: shinsaku@t.soka.ac.jp

Abbreviations: S-1, myosin subfragment-1; ABDF, 4-fluoro-7-sulfamoylbenzofurazan; ABD, 7-sulfamoylbenzofurazan4-yl; MIANS, 2-(4′-maleimidylanilino)naphthalene-6-sulfonic acid; TNBS, 2,4,6-trinitrobenzenesulfonate; DNP, dinitrophenyl; FDNB, 1-fluoro-2,4-dinitro-benzene; RLR, highly reactive lysine residue; SH1, reactive sulfhydryl-1 at Cys 707; SH2, reactive sulfhydryl-1 at Cys 697; $AlF_4^-$, aluminum fluoride; BeFn, beryllium fluoride; ScFn, scandium fluoride; $V_i$, orthovanadate; DTT, dithiothreitol; SDS-PAGE, sodium dodecyl sulfate-polyacrylamide gel electrophoresis.

suggest that the crystal structures may not reflect the actual conformation of myosin in solution. For instance, the $V_1$ and $AlF_4^-$ complexes are thought to correspond to the M**·ADP·$P_i$ state; yet their crystal structures suggest that the cystein region forms a helix, and therefore, the distance between the reactive cystein residues, Cys 707 and Cys 697, is identical to that of non-nucleotide myosin (*21, 22, 23*). Nevertheless, cross-linking experiments revealed that the distance between Cys 707 and Cys 697 is reduced from 12-14 to 3-5 Å during ATP hydrolysis (*7, 8*). With respect to the BeFn complex, analysis of tryptophan fluorescence enhancement as well as its interactions with actin indicate that it is certainly different from the non-nucleotide state (*14-16*). Furthermore, the most likely constitutively flexible regions of methylated skeletal muscle myosin head are loops 204-216 and 627-646, located at the junctions of the 25- and 50-kDa fragments and the 50- and 20-kDa fragments, respectively, but the loops can not be seen in crystal structures (*20*). Although crystallographic studies have provided details clarifying the exact structure of myosin, biochemical and fluorescence studies involving chemical modification of myosin remain very useful methods for investigating the role of conformational changes at flexible regions in the process of energy transduction.

It is well established that the reactivity of the sulfhydryl groups on Cys 707 (SH1) and Cys 697 (SH2) are very sensitive to nucleotide binding. Moreover, these residues can be crosslinked by a variety of bifunctional reagents having different spans (*6-8*), and in the swinging-neck model of muscle contraction, this flexible region has been identified as a fulcrum point (*24*). Based on analysis of the behavior of fluorescent probes, Hiratsuka speculated that the SH1-SH2 region acts as an energy transduction loop through which intersite communication between the ATP and actin binding sites is transmitted and suggested that the sequence of transient intermediates may be reflected in the changing conformation of the SH1-SH2 region (*25*).

Labeling SH1 and SH2 with the fluorescence dyes 4-fluoro-7-sulfamoylbenzofurazan (ABDF; *25*) and maleimide, 2-(4′-maleimidyanilino)naphthalene-6-sulfonic acid (MIANS; *26*), respectively, has proven useful for monitoring the conformational changes associated with ATP hydrolysis. The myosin head also contains a highly reactive lysine residue (RLR; Lys 83), which is rapidly and stoichiometrically modified by trinitrobenzene-sulfonate (TNBS; *27*). Trinitrophenylation of RLR changes the enzymatic properties of myosin; in the presence of $PP_i$ and nucleotide, trinitrophenylation of RLR is markedly reduced (*9-11, 28*), suggesting that the conformation of the RLR region is altered during hydrolysis of ATP. Thus, selective chemical modification of specific amino acid residues in myosin is likely to be useful for detecting localized conformational changes. In the present study, additional information about the transient states of myosin during the ATPase cycle were obtained by characterizing the conformational changes in the SH1, SH2, and RLR regions of $AlF_4^-$, BeFn, and ScFn ternary complexes.

## MATERIALS AND METHODS

*Proteins and Chemicals*—Myosin was prepared from chicken breast muscle by the method of Perry (*29*); the isolated myosin was then digested by $\alpha$-chymotrypsin to obtain subfragment-1 (S-1) as described by Weeds and Taylor (*30*). MIANS and ABDF were purchased from Molecular Probes (Eugene, OR, USA).

*ABDF Labeling of S-1*—Fluorescent labeling of S-1 with ABDF was carried out by reacting 10 $\mu$M S-1 and 30 $\mu$M ABDF in the presence of 20 mM cacodylate (pH 7.3) and 30 mM KCl for 1 h at 4°C in the dark. The reaction was stopped by addition of dithiothreitol (DTT) to a final concentration of 20 mM. The labeled S-1 was then passed through Sephadex G-50 column equilibrated with 30 mM Tris-HCl (pH 8.0) and 120 mM NaCl. The stoichiometry of the incorporated ABD group/S-1 was determined from the absorption spectrum using an extinction coefficient of 6,000 $M^{-1}\cdot cm^{-1}$ at 378 nm. Quantitative analysis of ABD-S-1 was performed using Coomassie plus protein assay reagent (PIERCE).

*MIANS Labeling of S-1*—Initially, S-1 was blocked by reacting 40 $\mu$M S-1 with 160 $\mu$M 2,4-dinitro-1-fluorobenzene (FDNB) in the presence of 0.5 M KCl, 50 mM Tris-HCl (pH 7.8), 2 mM $MgCl_2$, and 1 mM ADP for 20 min on ice. The blocked S-1 was then passed through Sephadex G-50 column equilibrated with 30 mM Tris-HCl (pH 7.5) and 120 mM NaCl. Blocked S-1 (20 $\mu$M) was then reacted with 26 $\mu$M MIANS in the presence of 30 mM KCl, 25 mM Tris-HCl (pH 7.8), 2.5 mM $MgCl_2$, and 1 mM ADP for 30 min at 4°C in the dark; the reaction was stopped by the addition of 10 mM DTT. The DNP group was then removed from S-1 by a further overnight incubation with 10 mM DTT at 4°C in the dark. The MIANS-S-1 was then passed through a Sephadex G-50 column equilibrated with 30 mM Tris-HCl (pH 8.0) and 120 mM NaCl. The stoichiometry of the incorporated MIANS groups/S-1 was determined from the differences in the absorption spectra of MIANS-S-1 and unlabeled S-1 using an extinction coefficient of $1.7\times10^4$ $M^{-1}\cdot cm^{-1}$ at 318 nm. The concentration of MIANS-S-1 was determined using Coomassie plus protein assay reagent (PIERCE).

*Fluorescence Measurements*—Fluorescence measurements were made at 25°C with an RF-5000 Spectrofluorometer (Shimadzu).

*Trinitrophenylation of S-1·ADP·$P_i$ Analogue Complexes*—S-1 (12 $\mu$M) was reacted with 0.25 mM trinitrobenzene-sulfonate at 25°C in 100 mM imidazole-HCl (pH 7.0), 0.5 M KCl, 5 mM $MgCl_2$ (or 5 mM $CaCl_2$) in the presence of 2 mM ATP, 2 mM ADP, or 2 mM ADP+1 mM BeFn ($AlF_4^-$ or ScFn). The time course of trinitrophenylation was monitored at 345 nm using a spectrophotometer equipped with a temperature-controlled cell (Shimadzu UV 2200).

## RESULTS

*ABDF Labeling of SH1 and Measurement of Fluorescence Emitted by Labeled S-1·ADP·Fluorometal Complexes*—In order to monitor conformational changes in the SH1 region, SH1 was selectively labeled with ABDF. Specific labeling of SH1 was confirmed by determining changes in the $Ca^{2+}$ and $K^+$-EDTA-ATPase activities that are characteristic of SH1 modification by ABDF. Figure 1 illustrates the increase in $Ca^{2+}$-ATPase activity and decrease in EDTA($K^+$)-ATPase activity. Changes in the ATPase activities reached respective plateaus when incorporation be-

came stoichiometric. These effects of ABDF labeling on ATPase activity were similar to those previously reported by Hiratsuka (*25*). Furthermore, following limited trypsin digestion, SDS-PAGE of S-1 labeled with ABDF (0.8–0.9 mol/mol S-1) revealed that only the SH1 region on the 20-kDa fragment was labeled; no labeling occurred on the 25- or 50-kDa fragments (not shown). ABDF-labeled S-1 (ABD-S-1) was then isolated from excess reagent and used in later experiments.

Time-dependent changes in the intensity of ABD-S-1 fluorescence were monitored after adding ATP, ADP, or ATP analogues. When ATP was added to a solution of ABD-S-1, fluorescence rapidly increased by 110% and remained at that level until all of the ATP was hydrolyzed to ADP; fluorescence then declined to levels typically elicited by ADP (Fig. 2). Due to formation of the stable ternary complex, S-1·ADP·BeFn, addition of ADP+BeFn rapidly increased ABD-S-1 fluorescence to the same levels as were seen with ATP, at which point, fluorescence intensity stabilized for up to 100 min. Another ternary complex, S-1·ADP·$AlF_4^-$, was formed when ABD-S-1 was exposed to ADP+$AlF_4^-$. The effect of its formation on ABD-S-1 fluorescence was quantitatively similar to the effect of S-1·ADP·BeFn formation, but the rate of rise in fluorescence intensity was much slower than was seen with either S-1·ADP·BeFn or ATP. Similarly, the addition of ADP+ScFn to ABD-S-1 resulted in a relatively slow increase in fluorescence intensity, although the rate was about 3 times faster than with ADP+$AlF_4^-$. On the other hand, the ATP analogues, 8-$N_3$-ATP and 8-Br-ATP, increased ABD-S-1 fluorescence to levels identical to those seen in the presence of ADP (53%; not shown). Interestingly, 8-$N_3$-ATP and 8-Br-ATP preferentially form the "syn" conformation with respect to *N*-glycoside bonds and do not induce contraction.

The rates of increase in ABD-S-1 fluorescence resulting from formation of fluorometal ternary complexes were consistent with our earlier analysis of the effect of ternary complex formation on enhanced intrinsic tryptophan fluorescence (*14*). Moreover, enhancement of intrinsic tryptophan fluorescence induced by 8-Br-ATP was identical to that in the presence of ADP (Table I). Thus, the conformational changes induced by these ATP analogues at the SH1 region appear to correspond to additional changes in the region of the tryptophan residues.

*MIANS Labeling of SH2 and Measurement of Fluorescence Intensities of S-1·ADP·Fluorometal Complexes*—Conformational changes at SH2 induced by the formation of ternary complexes were monitored by labeling SH2 with the environmentally sensitive fluorescent dye MIANS, according to the methods of Hiratsuka (*26*). In order to selectively label SH2, SH1 was initially blocked by FDNP. The DNP-S-1 was then labeled with MIANS at SH2 in the presence of $Mg^{2+}$-ADP. The DNP group on SH1 was then removed by thiolysis using DTT. Specific SH2 labeling was confirmed by measuring ATPase activity, and stoichiometric labeling was estimated from the MIANS extinction coefficient. The relationship between the percentage of remaining ATPase activities of MIANS-S-1 and the number of MIANS groups/S-1 is shown in Fig. 3. The changes in $Mg^{2+}$-, $Ca^{2+}$-, and $K^+$-ATPase activities exhibited the characteristic patterns associated with labeling of SH2 previously reported by Hiratsuka (*26*)—increased $Mg^{2+}$-ATPase activity, decreased $K^+$-ATPase activity, and little

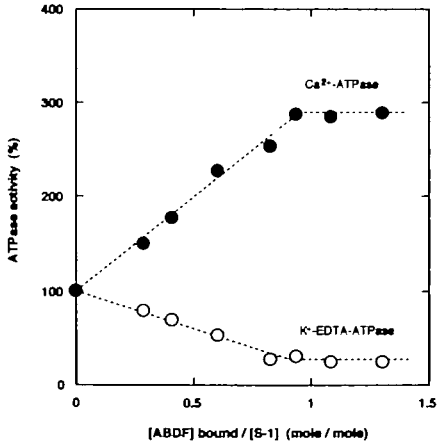


Fig. 1. **EDTA($K^+$)-ATPase and $Ca^{2+}$-ATPase activities of S-1 labeled with ABDF at SH1.** Labeled S-1 was prepared as described in "MATERIALS AND METHODS." EDTA($K^+$)-ATPase (○) and $Ca^{2+}$-ATPase (●) activities were measured at 25°C in 1 mM ATP, 0.5 M KCl, and 50 mM Tris-HCl (pH 8.0) in the presence of 5 mM EDTA and $CaCl_2$, respectively. The reaction was stopped by addition of 10% trichloroacetic acid and the released $P_i$ was determined by the method of Youngburg and Youngburg (*36*). The number of labeled thiol groups/S-1 was determined by the method of Ellman (*35*).

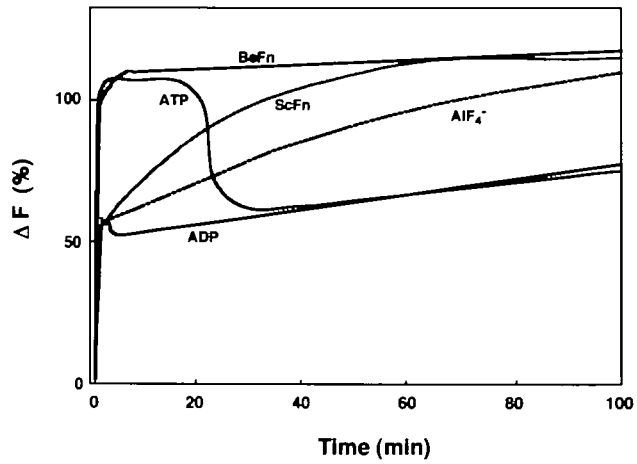


Fig. 2. **Time-dependent changes in ABD-S-1 fluorescence following addition of ADP and $P_i$ analogues.** To ABD-S-1 (5 $\mu$M) in solution with 120 mM NaCl, 30 mM Tris-HCl (pH 7.5), and 2 mM $MgCl_2$ was added 25 $\mu$M ATP, 1 mM ADP, or 1 mM ADP+1 mM BeFn, $AlF_4^-$, or ScFn. Fluorescent emission was monitored at 500 nm (excitation at 390 nm).

TABLE I. **Tryptophan fluorescence enhancement of S-1 induced by formation of ternary complexes.** Fluorescence was measured in 50 mM KCl, 30 mM Tris-HCl pH 7.5, 2 mM $MgCl_2$. Excitation at 300 nm; emission at 340 nm.

| Complexes | Fluorescence change $\Delta F_{max}/F$ (%) |
|---|---|
| S-1·ADP·$AlF_4^-$ | 17 |
| S-1·ADP·BeFn | 12 |
| S-1·ADP·ScFn | 17 |
| S-1·8-Br-ATP | 5 |
| S-1·ATP | 16 |
| S-1·ADP | 5 |

or no change in $Ca^{2+}$-ATPase activity. When incorporation of MIANS into S-1 exceeded stoichiometric labeling, $Mg^{2+}$- and $Ca^{2+}$-ATPase activities declined, suggesting the labeling was becoming increasingly nonspecific. To minimize fluorescence from nonspecific labeling, our experiments were conducted using S-1 labeled with 0.8–0.9 mol of MIANS/mol S-1 (Fig. 3). When ATP was added to a solution of MIANS-S-1, the fluorescence intensity decreased to about 65% of that seen in the absence of ATP. After the ATP was hydrolyzed to ADP, fluorescence intensity increased to 75%, which was identical to fluorescence elicited by addition of ADP.

Figure 4A shows the fluorescence changes induced by adding of ADP+phosphate analogues. As expected, addition of ADP decreased fluorescence to 75% of non-nucleotide levels. Thereafter, phosphate analogues were added to characterize the fluorescence changes resulting from formation of ternary complexes. In the presence of ADP+BeFn, fluorescence decreased to 65%, which is identical to the intensity seen in the presence of ATP. In contrast, fluorescence intensities were unaffected by the addition ScFn or $AlF_4^-$ to solutions containing MIANS-S-1 and ADP, even after 140 min of incubation.

Because the fluorescence change of in the presence of ADP+$AlF_4^-$ or ScFn proved to be identical to those elicited by ADP alone, it was important to verify that $AlF_4^-$ and ScFn were able to bind to MIANS-S-1. To accomplish this, formation of ScFn and $AlF_4^-$ ternary complexes was examined by measuring the time-dependent inhibition of ATPase activity induced by preincubation of MIANS-S-1 and unmodified S-1 with $Mg^{2+}$-ADP+$AlF_4^-$ or ScFn. As shown in Fig. 5, incubation with $AlF_4^-$ completely blocked MIANS-S-1 ATPase activity within 60 min; inhibition of unmodified S-1 developed at approximately the same rate. The effects of ScFn on the ATPase activities of MIANS-S-1 and unmodified S-1 were similar, although the inhibition developed more slowly than with $AlF_4^-$. These results clearly indicate that the MIANS-S-1 forms ternary complexes with ADP and $AlF_4^-$ or ScFn as readily as does native S-1.

The effects of $V_I$ were also examined and compared with the results of other complexes. The absorption maximum for $V_I$ is about the same as the excitation wavelength of MIANS. Consequently, $V_I$ elicited an apparent concentration-dependent decline in MIANS-S-1 fluorescence intensity (Fig. 4B). Subsequent addition of ADP elicited further declines in fluorescence. In the presence of $V_I$, addition of excess ATP did not change fluorescence intensity, presumably because the active sites were already occupied by ADP-$V_I$.

*Trinitrophenylation of RLR in S-1·ADP·Fluorometal Complexes*—We examined RLR reactivity in S-1·ADP·fluorometal complexes and compared the reactivity in the presence of ADP and ATP alone. In the presence of ADP, the rate of trinitrophenylation was reduced to ~50% of that seen in the absence of nucleotide (Fig. 6), which is similar to previous reports (*9, 10*), and trinitrophenylation was

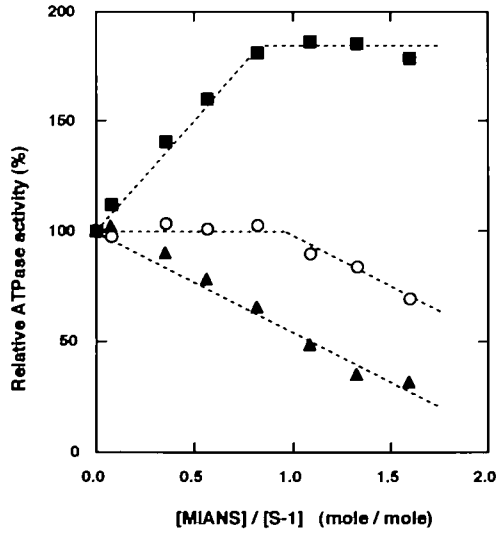


Fig. 3. **Effect of the MIANS labeling on relative ATPase activities.** ATPase activity was measured at 25°C in the presence of 1 $\mu$M MIANS-S-1, 0.5 M KCl, 30 mM Tris-HCl (pH 7.5), and 2 mM ATP. For the measurement of $Mg^{2+}$-ATPase activity (■), $Ca^{2+}$-ATPase activity (○), and EDTA($K^+$)-ATPase activity (▲), $MgCl_2$, $CaCl_2$, or EDTA was added to the respective mixtures to a final concentration of 5 mM.

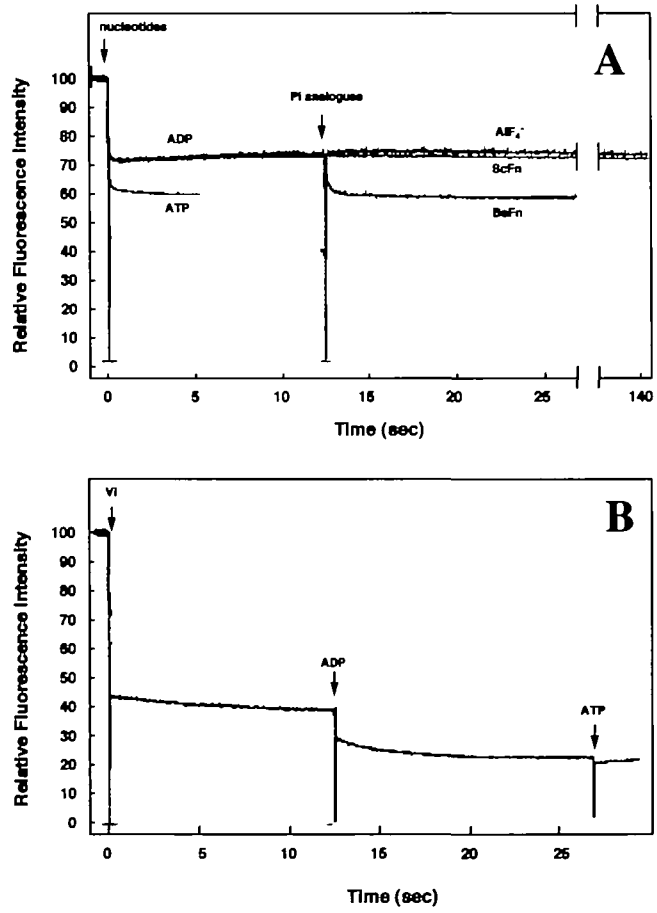


Fig. 4. **Time courses of the decline in MIANS-S-1 fluorescence induced by ADP and $P_i$ analogues.** (A) 0.5 mM ATP, 1 mM ADP or 1 mM ADP+1 mM BeFn, $AlF_4^-$, or ScFn were added to solutions containing 1 $\mu$M MIANS-S-1, 120 mM NaCl, 30 mM Tris-HCl (pH 7.5), and 2 mM $MgCl_2$. (B) To the MIANS-S-1 solution, 1 mM $V_I$ was added first, then 1 mM ADP was added. Changes in MIANS-S1 fluorescence were measured at 420 nm (excitation at 330 nm).

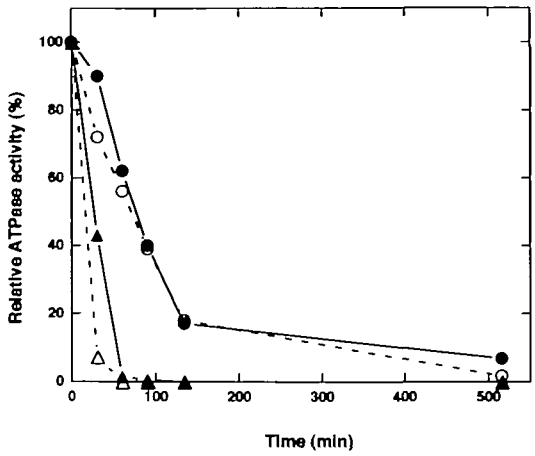


Fig. 5. **Time-dependent inhibition of MIANS-S-1 ATPase activity by $AlF_4^-$ and ScFn:** MIANS-S-1 or S-1 were incubated at 25°C in the presence of 120 mM NaCl, 30 mM Tris-HCl (pH 7.5), 1 mM $MgCl_2$, 1 mM ADP, and 1 mM $AlF_4^-$ or 0.2 mM ScFn. EDTA-($K^+$)-ATPase activity was then measured at selected times in the presence of 0.1 $\mu$M MIANS-S-1 or S-1, 0.5 M KCl, 30 mM Tris-HCl (pH 7.5), 6 mM EDTA, and 2 mM ATP at 25°C. MIANS-S-1:ScFn (●), S-1:ScFn (○), MIANS-S-1:$AlF_4^-$ (▲), S-1:$AlF_4^-$ (△).

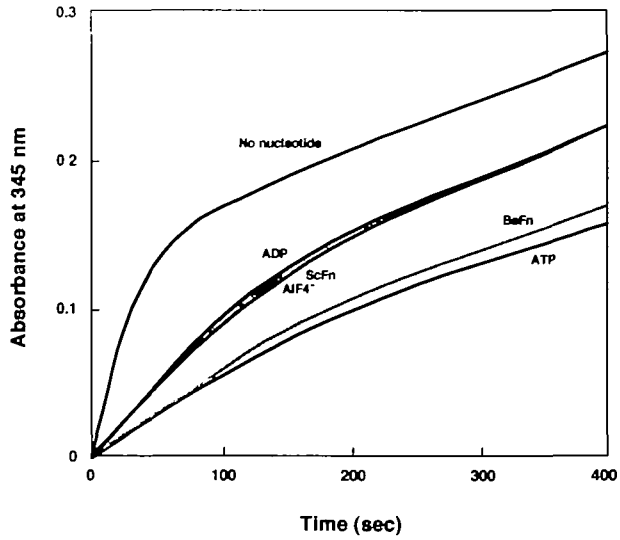


Fig. 6. **Time course of trinitrophenylation of S-1 with ATP analogues.** S-1 (12 $\mu$M) was reacted with trinitrobenzene-sulfonate (0.25 mM) at 25°C in 100 mM imidazole-HCl (pH 7.0), 0.5 M KCl, 5 mM $MgCl_2$ (or 5 mM $CaCl_2$) in the presence of 2 mM ATP, 2 mM ADP or 2 mM ADP+1 mM BeFn, $AlF_4^-$ or ScFn.

completely blocked by addition of ATP. ADP+BeFn also completely inhibited trinitrophenylation of RLR in the same manner as ATP, suggesting that, in the S-1•ADP•BeFn complex, the local conformation at or near Lys 83 resembles the conformation in the presence of ATP. In contrast, ADP+$AlF_4^-$ or ScFn reduced trinitrophenylation to the same level as seen in the presence of ADP alone. Thus, in the presence of $AlF_4^-$ or ScFn ternary complexes, the local conformation in the region of RLR does not correspond to formation of M**•ADP•$P_i$.

## DISCUSSION

ABDF is a reagent that reacts vigorously and selectively with SH1. It was originally shown by Hiratsuka (*25*) that the fluorescence emission spectrum of ABD-S-1 was very sensitive to ATP-induced conformational changes at SH1. For this reason, specific labeling at SH1 was carried out according to the methods described by Hiratsuka (*25*) and monitored by measuring ATPase activity (Fig. 1). Elevation of $Ca^{2+}$-ATPase activity and reduction of EDTA($K^+$)-ATPase activity, corresponding to incorporation of the ABD group, revealed specific labeling at SH1 but not SH2.

Upon addition of $Mg^{2+}$-ATP, myosin quickly forms the myosin**•ADP•$P_i$ intermediate; this reaction is characterized by an increase in the intrinsic tryptophan fluorescence intensity (*31*). Increases in ABD-S-1 fluorescence were also associated with enhanced intrinsic tryptophan fluorescence as shown in Fig. 2 and Table I. Thus, the conformational changes at SH1 induced by ternary complex formation appear to correspond to the conformational changes at the tryptophan which occur when ATP binds. Trp 510 has been identified as the residue contributing most to the enhanced fluorescence (*37, 38*). This means that the 110% increase in ABD-labeled SH1 fluorescence may reflect formation of the M**•ADP•$P_i$ state. Consistent with this notion, addition of 8-Br-ATP or 8-$N_3$-ATP, which do not induce superprecipitation, sliding of actin filaments, or tryptophan fluorescence enhancement (*32*), only increased ABD-S-1 fluorescence slightly. Addition of ADP+BeFn rapidly increased ABD-S-1 fluorescence until it was virtually identical to the intensities seen in the presence of ATP. Although increases in fluorescence elicited by addition of ADP+ScFn or $AlF_4^-$ developed more slowly, ultimately, the fluorescence attained the same intensity as seen in the presence of ATP. Moreover, the time required to reach maximum fluorescence was consistent with the time needed to form the ternary complexes (*14, 16, 18*). For example, the time of approximately 60 min to reach maximum fluorescence in the presence of ADP+ScFn (Fig. 2) is consistent with the time required to form the S-1•ADP•ScFn ternary complex estimated from ATPase inhibition (*18*). These results suggest that for all of the complexes, the local conformations at SH1 are similar to that of the M**•ADP•$P_i$ state.

The aforementioned observations differ from those of Phan *et al.* (*19*), who also chemically modified SH1 using fluorescent probes and who reported that the structure of the BeFn complex resembles that of the M*•ATP state. Despite this finding, in the present study the BeFn complex exhibited enhanced tryptophan fluorescence which was almost identical to that seen in the presence of ATP *i.e.*, M**•ADP•$P_i$ (*14, 15*). Furthermore, recent small angle X-ray scattering studies clearly demonstrated that the shape of the S-1•ADP•BeFn complex is rounded or bend in the same manner as S-1 is bent in the presence of ATP (*13*). Thus, current evidence suggests it is more likely that the S-1•ADP•BeFn complex resembles the M**•ADP•$P_i$ state than the M*•ATP state. Finally, very recent crystallographic studies of the BeFn complex of truncated *Dictyostelium* S-1 (Holmes, K., unpublished observation) and smooth muscle myosin (Dominguez, R., Freyzon, Y., Trybus, K., and Cohen, C., unpublished observation) also showed rounded or compact global structure, in contrast with the structure reported by Rayment *et al.* (*20*).

While the discrepancies in the results are unclear, it may

be possible for the S-1·ADP·BeFn complex to mimic both the M**·ADP·$P_i$ and M*·ATP states. Using $^{19}$F-NMR, it was demonstrated that, in solution, the BeFn incorporated into ternary complexes exist as at least four species (*33*). Moreover, the $^{19}$F-NMR spectrum of a $^{19}$F-labeled ADP analogue, trapped into skeletal muscle myosin S-1 with BeFn, indicates that two distinct conformations exist at the ATPase site (*34*). It is proposed that the various species of BeFn are distinct from each other in their character, and the ternary complexes composed of these species may mimic different states in the ATPase cycle. The population of the species (ratio of Be:F) may be affected by factors such as reagent concentration and pH, and it may be possible that the distinct species of S-1·ADP·BeFn complex are crystallized.

In contrast to SH1, the local conformation at SH2 reflected the differences between the ternary complexes of $AlF_4^-$, ScFn, and BeFn. As shown in Fig. 4A, fluorescence emitted by the MIANS-S-1·ADP·$AlF_4^-$ or ScFn complexes was similar to that emitted in presence of ADP (Fig. 6). In contrast, the fluorescence intensity of the MIANS-S-1·ADP·BeFn complex was identical to that seen in the presence of ATP. From the data shown in Fig. 4B, we concluded that the conformation of the MIANS-S-1·ADP·$V_i$ complex at SH2 is also similar to that which exists in the presence of ATP. Thus, the local conformation at SH2 of the S-1·ADP·$AlF_4^-$ or ScFn complex is distinct from that of the S-1·ADP·BeFn or $V_i$ complex.

Conformational changes at SH2 may not be accompanied by formation of the M**·ADP·$P_i$ state as is the case with conformational changes at SH1. Experimental data show that 8-$N_3$-ATP, 8-Br-ATP, and $Ca^{2+}$-ATP, which are all hydrolyzed by myosin without formation of the M**·ADP·$P_i$ state, increase tryptophan fluorescence very slightly. However, 8-$N_3$-ATP, 8-Br-ATP, and $Ca^{2+}$-ATP completely attenuated MIANS-S-1 fluorescence and are all able to dissociate acto-myosin (*32*). Therefore, local conformational changes at SH2 may be communicated by changes at the actin binding site. We suggest that the conformation at SH2 may correspond to a transient state occurring earlier than the M**·ADP·$P_i$ state, perhaps at or near the M*·ATP state.

Altered RLR reactivity resulting from formation of ternary complexes and reflecting the local conformation in the RLR region was associated with corresponding changes in MIANS-S-1 fluorescence. As shown in Fig. 6, in the presence of ADP+$AlF_4^-$ or ScFn, the RLR reactivity was reduced to about 50% and was the same as that seen with ADP. Complete inhibition of reactivity in the presence of ADP+BeFn indicates that the conformation at the RLR region of the S-1·ADP·BeFn complex is different from that of the S-1·ADP·$AlF_4^-$ or ScFn complex.

In the present study, we demonstrated that the local conformation in the SH2 region of the S-1·ADP·BeFn complex is different from local SH2 conformations in the S-1·ADP·$AlF_4^-$ and ScFn complexes. The two highly reactive sulfhydryl groups, SH1 and SH2, *i.e.*, Cys 707 and Cys 697, respectively, appear to move distinctly during the ATPase cycle. It was also shown that the SH1 region is responsive to formation of the M**·ADP·$P_i$ state, and the SH2 region reflects conformational changes corresponding to dissociation of actomyosin. Conformational changes in the RLR region are also associated with changes in the SH2 regions. Finally, these results support the idea that the respective ternary complexes correspond to analogues of different transient states in the ATPase cycle.

## REFERENCES


1. Hibberd, M. and Trentham, D.R. (1986) Relationships between chemical and mechanical events during muscular contraction. *Annu. Rev. Biophys. Biophys. Chem.* **15**, 119-161
2. Dantzig, J.A., Goldman, Y.E., Millar, N.C., Lacktis, J., and Homsher, E. (1992) Reversal of the cross-bridge force-generating transition by photogeneration of phosphate in rabbit psoas muscle fibres. *J. Physiol.* **451**, 247-248
3. Johnson, W.C., Jr., Bivin, D.B., Ue, K., and Morales, M.F. (1991) A search for protein structural changes accompanying the contractile interaction. *Proc. Natl. Acad. Sci. USA* **88**, 9748-9750
4. Hiratsuka, T. (1992) Spatial proximity of ATP-sensitive tryptophanyl residue(s) and Cys-697 in myosin ATPase. *J. Biol. Chem.* **267**, 14949-14954
5. Park, S., Ajtai, K., and Burghardt, T.P. (1996) Optical activity of a nucleotide-sensitive tryptophan in myosin subfragment 1 during ATP hydrolysis. *Biophys. Chem.* **63**, 67-80
6. Cheung, H.C., Gryczynski, I., Malac, H., Wiczk, W., Johnson, M.L., and Lakowicz, J.R. (1991) Conformational flexibility of the Cys 697-Cys 707 segment of myosin subfragment-1. Distance distributions by frequency-domain fluorometry. *Biophys. Chem.* **40**, 1-17
7. Reisler, E., Burke, M., Himmelfarb, S., and Harrington, W.F. (1974) Spatial proximity of the two essential sulfhydryl groups of myosin. *Biochemistry* **13**, 3837-3840
8. Wells, J.A. and Yount, R.G. (1982) Chemical modification of myosin by active-site trapping of metal-nucleotides with thiol crosslinking reagents. *Methods Enzymol.* **85**, 93-116
9. Miyanishi, T., Inoue, A., and Tonomura, Y. (1979) Differential modification of specific lysine residues in the two kinds of subfragment-1 of myosin with 2,4,6-trinitrobenzenesulfonate. *J. Biochem.* **85**, 747-753
10. Komatsu, H., Emoto, Y., and Tawada, K. (1993) Half-stoichiometric trinitrophenylation of myosin subfragment 1 in the presence of pyrophosphate or adenosine diphosphate. *J. Biol. Chem.* **268**, 7799-7808
11. Mornet, D., Pantel, P., Bertrand, R., Audemard, E., and Kassab, R. (1980) Localization of the reactive trinitrophenylated lysyl residue of myosin ATPase site in the $NH_2$-terminal (27 k domain) of S1 heavy chain. *FEBS Lett.* **17**, 183-188
12. Wakabayashi, K., Tokunaga, M., Kohno, I., Sugimoto, Y., Hamanaka, T., Takezawa, Y., Wakabayashi, T., and Amemiya, Y. (1992) Small-angle synchrotron X-ray scattering reveals distinct shape changes of the myosin head during hydrolysis of ATP. *Science* **258**, 443-447
13. Sugimoto, Y., Tokunaga, M., Takezawa, Y., Ikebe, M., and Wakabayashi, K. (1995) Conformational changes of the myosin head during hydrolysis of ATP as analyzed by X-ray solution scattering. *Biophys. J.* **68**, 29s-34s
14. Maruta, S., Henry, G.D., Sykes, B.D., and Ikebe, M. (1993) Formation of the stable myosin-ADP-aluminum fluoride and myosin-ADP-beryllium fluoride complex and their analysis using $^{19}$F-NMR. *J. Biol. Chem.* **268**, 7093-7100
15. Werber, M.M., Peyser, Y.M., and Muhlrad, A. (1992) Characterization of stable beryllium fluoride, aluminum fluoride, and vanadate containing myosin subfragment 1-nucleotide complexes. *Biochemistry* **31**, 7190-7197
16. Phan, B. and Reisler, E. (1992) Inhibition of myosin ATPase by beryllium fluoride. *Biochemistry* **31**, 4787-4793
17. Goodno, C.C. (1979) Inhibition of myosin ATPase by vanadate ion. *Proc. Natl. Acad. Sci. USA* **76**, 2620-2624
18. Gopal, D. and Burke, M. (1995) Formation of stable inhibitory complexes of myosin subfragment 1 using fluoroscandium anions. *J. Biol. Chem.* **270**, 19282-19286
19. Phan, B.C., Peyser, Y.M., Reisler, E., and Muhlrad, A. (1997)

Effect of complexes of ADP and phosphate analogs on the conformation of the Cys 707-Cys 697 region of myosin subfragment 1. *Eur. J. Biochem.* **243**, 636-642
20. Rayment, I., Rypniewski, W.R., Schmidt-Bäse, K., Smith, R., Tomchick, D., Benning, M.M., Winkelman, D.A., Wesenberg, G., and Holden, H.M. (1993) Three-dimensional structure of myosin subfragment-1: a molecular motor. *Science* **261**, 50-58
21. Smith, C.A. and Rayment, I. (1995) X-ray structure of the magnesium (II)-pyrophosphate complex of the truncated head of *Dictyostelium discoideum* myosin to 2.7 Å resolution. *Biochemistry* **34**, 8973-8981
22. Fisher, A.J., Smith, C.A., Thoden, J.B., Smith, R., Sutoh, K., Holden, H.M., and Rayment, I. (1995) X-ray structures of the myosin motor domain of *Dictyostelium discoideum* complexed with MgADP·BeFx and MgADP·$AlF_4^-$. *Biochemistry* **34**, 8960-8972
23. Smith, C.A. and Rayment, I. (1996) X-ray structure of the magnesium (II)· ADP·vanadate complex of the *Dictyostelium discoideum* myosin motor domain to 1.9 Å resolution. *Biochemistry* **35**, 5404-5417
24. Uyeda, T.Q.P., Abramson, P.D., and Spudich, J.A. (1996) The neck region of the myosin motor domain acts as a lever arm to generate movement. *Proc. Natl. Acad. Sci. USA* **93**, 4459-4464
25. Hiratsuka, T. (1993) Behavior of Cys-707 (SH1) in myosin associated with ATP hydrolysis revealed with a fluorescent probe linked directly to the sulfur atom. *J. Biol. Chem.* **268**, 24742-24750
26. Hiratsuka, T. (1992) Movement of Cys-697 in myosin ATPase associated with ATP hydrolysis. *J. Biol. Chem.* **267**, 14941-14948
27. Kubo, S., Tokura, S., and Tonomura, Y. (1960) *J. Biol. Chem.* **235**, 2835-2839
28. Setton, A. and Muhlrad, A. (1988) The effect of pyrophosphate on the reaction of myosin with 2,4,6-trinitrobenzene sulphonate. *J. Muscle Res. Cell Motil.* **9**, 132-146
29. Perry, S.V. (1952) Myosin adenosine triphosphatase. *Methods Enzymol.* **2**, 582-588
30. Weeds, A.G. and Taylor, R.S. (1975) Separation of subfragment-1 isozymes from rabbit skeletal muscle myosin. *Nature* **257**, 54-56
31. Weber, M.M., Szent-Gyorgyi, A.G., and Fasman, G.D. (1972) Fluorescence studies on heavy meromyosin-substrate interaction. *Biochemistry* **11**, 2872-2883
32. Maruta, S. and Ohki, T. (1996) Conformational change on myosin head induced by binding of ATP analogue which has "syn" conformation at *N*-glycoside bond. *Biophys. J.* **70**, 264a
33. Henry, G.D., Maruta, S., Ikebe, M., and Sykes, B.D. (1993) Observation of multiple myosin subfragment-1:ADP:fluoroberyllate complexes by $^{19}$F-NMR. *Biochemistry* **32**, 10451-10456
34. Maruta, S., Henry, G.D., Sykes, B.D., and Ikebe, M. (1998) Analysis of stress in the active site of myosin accompanied by conformational changes in transient state intermediate complexes using photoaffinity labeling and $^{19}$F-NMR spectroscopy. *Eur. J. Biochem.* **252**, 520-529
35. Ellman, G.L. (1959) Tissue sulfhydryl groups. *Arch. Biochem. Biophys.* **82**, 70-77
36. Youngburg, G.E. and Youngburg, M.V. (1930) Phosphorus metabolism: I. A system of blood phosphorus analysis. *J. Lab. Clin. Med.* **16**, 158-166
37. Bivin, D.B., Kubota, S., Pearlstein, R., and Morales, M.F. (1993) On how a myosin tryptophan may be perturbed. *Proc. Natl. Acad. Sci. USA* **90**, 6791-6795
38. Hiratsuka, T. (1992) Spatial proximity of ATP-sensitive tryptophanyl residue(s) and Cys-697 in myosin ATPase. *J. Biol. Chem.* **267**, 14949-14954